Science of the Total Environment 853 (2022) 158701

Contents lists available at ScienceDirect

Science of the Total Environment

journal homepage: www.elsevier.com/locate/scitotenv

Experimental assessment of tundra fire impact on element export and storage in permafrost peatlands

Daria Kuzmina [a], Artem G. Lim [a], Sergey V. Loiko [a], Oleg S. Pokrovsky [b,c,*]

[a] BIO-GEO-CLIM Laboratory, Tomsk State University, 36 av. Lenina, Tomsk 634004, Russia
[b] GET UMR 5563 CNRS University of Toulouse, 14 Avenue Edouard Belin, 31400 Toulouse, France
[c] N Laverov Federal Center for Integrated Arctic Research, Ural Branch of the Russian Academy of Science, 23 Nab Severnoi Dviny, Arkhangelsk 163000, Russia

HIGHLIGHTS

- Laboratory study of ash from tundra vegetation.
- Peat, moss and lichen ashes rapidly released major and trace elements to the fluid.
- Moss ash released the highest amount of solutes.
- Negligible effect of tundra wildfire on riverine export and lake storage of nutrients and metals.

GRAPHICAL ABSTRACT

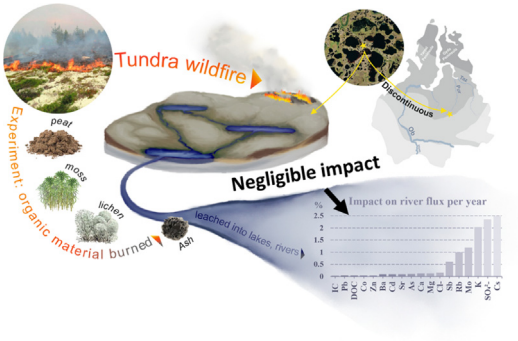

ARTICLE INFO

Editor: Manuel Esteban Lucas-Borja

Keywords:
Moss
Lichen
Peat
Ash
Nutrient
River

ABSTRACT

Extensive studies have been performed on wildfire impact on terrestrial and aquatic ecosystems in the taiga biome, however consequences of wildfires in the tundra biome remain poorly understood. In such a biome, permafrost peatlands occupy a sizable territory in the Northern Hemisphere and present an extensive and highly vulnerable storage of organic carbon. Here we used an experimental approach to model the impact of ash produced from burning of main tundra organic constituents (i.e., moss, lichen and peat) on surrounding aquatic ecosystems. We studied the chemical composition of aqueous leachates produced during short-term (1 week) interaction of ash with distilled water and organic-rich lake water at 5 g_{solid} L^{-1} and 20 °C. The addition of ash enriched the fluid phase in major cations (i.e., Na, Ca, Mg), macro- (i.e., P, K, Si) and micronutrients (i.e., Mn, Fe, Co, Ni, Zn, Mo). This enrichment occurred over <2 days of experiment. Among 3 studied substrates, moss ash released the largest amount of macro- and microcomponents into the aqueous solution. To place the obtained results in the environmental context of a peatbog watershed, we assume a fire return interval of 56 years and that the entire 0–10 cm of upper peat is subjected to fire impact. These mass balance calculations demonstrated that maximal possible delivery of elements from ash after soil burning to the hydrological network is negligibly small (<1–2 %) compared to the annual riverine export flux and element storage in thermokarst lakes. As such, even a 5–10 fold increase in tundra wildfire frequency may not sizably modify nutrient and metal fluxes and pools in the surrounding aquatic ecosystems. This result requires revisiting the current paradigm on the importance of wildfire impact on permafrost peatlands and calls a need for experimental work on other ecosystem compartments (litter, shrubs, frozen peat) which are subjected to fire events.

* Corresponding author at: GET UMR 5563 CNRS University of Toulouse (France), 14 Avenue Edouard Belin, 31400 Toulouse, France.
E-mail address: oleg.pokrovsky@get.omp.eu (O.S. Pokrovsky).

http://dx.doi.org/10.1016/j.scitotenv.2022.158701
Received 29 June 2022; Received in revised form 7 September 2022; Accepted 8 September 2022
Available online xxxx

1. Introduction

One of the biggest unknowns about climate warming in high latitudes is the response of wildfire area, fire frequency and fire severity (Flannigan et al., 2000; Kasischke et al., 2005, 2010; Ludwig et al., 2018). The global-scale effect of wildfires in the boreal and subarctic regions stems from large stocks of combustible materials on the forest floor, (i.e., plant litter, mosses and lichens) (Czimczik et al., 2003; Neff et al., 2005; Boby et al., 2010). For example, fires are the main destabilizing factor in the boreal belt of Siberia (Kasischke and Turetsky, 2006; Kharuk et al., 2021; Talucci et al., 2022). It has been documented that tundra fire is among the most important driving forces of permafrost carbon release into the atmosphere (Miner et al., 2022); this is especially true for the Western Siberian Lowland (WSL), a territory of forest, forest-tundra and peatlands that contains a vast amount of organic carbon (OC) in the form of peat and vegetation (Botch et al., 1995; Beilman et al., 2009).

Through consuming a sizable amount of ecosystem OC stock, wildfires accelerate the recycling of major and micronutrients such as K, S, N, P, Si and trace metals (Whelan, 1995; Moilanen et al., 2002; Spencer et al., 2003). Pyrogenic material (i.e., plant and topsoil ash) produced from the burning of organic matter constitutes a sizable pool of highly reactive materials which can profoundly affect soil physical and chemical properties. The magnitude of these impacts depends on temperature and duration of combustion, soil moisture content at time of burning and identity and chemical composition of the burning vegetation (Wright and Bailey, 1982; Grey and Dighton, 2006; White-Monsant et al., 2015). Tundra fires are known to strongly impact the carbon and element cycling in high latitudes (de Groot et al., 2013; Hanes et al., 2019; Chen et al., 2021). However, for application in forestry and available tree stand assessment, the overwhelming majority of experimental and natural studies in Siberia have dealt with forest rather than tundra vegetation (Ivanova et al., 2011; Larjavaara et al., 2017; Köster et al., 2018; Prokushkin et al., 2018; Knorre et al., 2019). Numerous studies on environmental impact of the tundra fire in other regions (Hu et al., 2015; Burd et al., 2018; Gibson et al., 2018; Heim et al., 2021) do not assess specific chemical mechanisms responsible for fire product leaching to surface waters. Moreover, relatively little is known about this important consequence of tundra wildfire with potential to modify the chemical composition of surrounding surface waters (thaw ponds and thermokarst lakes) and riverine element export from the watershed (Parham et al., 2013).

Ash produced during vegetation burning is rich in essential nutrients like nitrogen, sulfur, phosphorus and potassium (Koyama et al., 2010; Harden et al., 2004; Neff et al., 2005). Because most of these elements are present in a water-soluble state (Pereira et al., 2012), they are highly mobile over the first days to weeks after a wildfire has occurred (Christensen, 1973; Grier, 1975; Kaufmann et al., 1993). Fire-induced nutrient losses from terrestrial ecosystems with stream runoff (Bayley et al., 1992; Lamontagne et al., 2000; Petrone et al., 2007) are likely to be particularly important in permafrost-dominated regions with shallow soils and short residence time of water at the watershed (Ala-aho et al., 2018). In such regions, wildfires are capable of altering both stream chemistry and water column biological activity (Kawahigashi et al., 2011; Parham et al., 2013; Diemer et al., 2015; Rodríguez-Cardona et al., 2020).

This study aims to provide quantitative constraints on tundra vegetation (i.e., mosses and lichens) and peat ash reactivity in model aqueous solutions; these solutions imitate natural rainfall conditions and the organic-rich nature of surface water in permafrost peatlands. As a working hypothesis, we suggested that moss ash exhibits the highest reactivity in aqueous solutions. This hypothesis is based on recent results of mesocosm experiments with live vegetation in permafrost peatlands (Shirokova et al., 2021; Manasypov et al., 2017). A secondary hypothesis, in accord with the existing paradigm that the wildfire is among the most significant factors for climate warming impact on the biogeochemical cycle of elements in the permafrost regions (Abbott et al., 2016, 2021; Ackley et al., 2021), was that tundra wildfire is capable of strongly modifying element transfer between burned peat/soil and adjacent aquatic systems. To assess this, we compared the lateral export (yield) of major and trace elements from burned mosses, lichens and peat at the watershed scale to the annual riverine yield of nutrients, metals and dissolved element storage in thermokarst lakes.

Quantifying the magnitude of tundra vegetation and peat ash reactivity in naturally-relevant solutions should allow for a better prediction of the scale of impact that tundra wildfires have on the surrounding hydrological network. This information is greatly needed to foresee changes in element delivery from land to ocean amidst on-going climate changes and environmental disturbances in western Siberia and other global permafrost peatlands.

2. Methods

2.1. Moss, lichen and peat ash preparation

Sampling of peat, vegetation and lake water was performed in August 2020 at the Khanymey Research station (INTERACT Network), 63°47′N, 75°43′E. The upper peat horizon used in this study represented the first 0–10 cm of soil after removal of moss and litter. This is the typical peat depth affected by tundra fire according to Liljedahl et al. (2007). It was sampled at the peat mound and dried at 40 °C using Osmofilm® bags over 5 days. The peat was 5 to 10 % decomposed and contained 55 % lichens (40 % of *Cladonia stellaris* and 15 % of *Cladonia stygia*), 30 % dwarf shrubs, 15 % Sphagnum moss with some wood remnants, bark and pollens as determined by botanical analysis (Morgalev et al., 2017). The peat was slightly ground/disintegrated before subjecting to ashing. The apical (live) part of *Cladonia stellaris* and *Sphagnum fuscum*, highly abundant in the frozen mounds of the palsa peat bog at the Khanymey Research Station and constituting >90 % of peat mound surface vegetation (Volkova et al., 2018), were rinsed in Milli-Q water and dried in open air using Osmofilm® bags.

Approximately 80 g of dry peat, lichen or moss were placed in pre-cleaned porcelain cups and separately burned for 3 h at 525 °C in a Vecstar® furnace. This temperature corresponds to the upper range of in-situ temperatures recorded during tundra ground fire (Agafontsev and Kasymov, 2020) and was chosen to ensure maximal burning of organic material thereby representative of an extreme case of wildfire. The motivation for this choice was that, unlike organic-rich soils of flat peatlands subjected to smoldering (i.e., Benscoter et al., 2011), the permafrost palsa peatbogs investigated in the present study are represented by convex mounds that do not hold water and become extremely dry during summer time. The ash produced by this burning had a black color potentially indicating not a 100 % removal of OM (i.e., Bodí et al., 2014), as was also reflected in the small amount of residual organic carbon (mass loss 1 to 2.5 % after burning at 1200 °C). Note that recently, Li et al. (2022) demonstrated incomplete consumption of organic matter even at 525 °C. The ash mass content of dry peat, lichen and moss biomass was equal to 2.5 ± 0.5, 0.8 ± 0.1 and 1.8 ± 0.7 %, respectively, as measured by triplicate analysis.

2.2. Laboratory experiments on ash dissolution

For leaching experiments, sterile 0.22-μm filtered and UV-treated Milli-Q water and natural lake water were used. The lake water was collected in August 2020 from the surface of a thermokarst lake located at the Khanymey Research Station (11,000 m^2 surface area, depth 0.5–1.0 m) and immediately filtered through a sterile 0.45 μm Nalgene filtration unit and then stored at 4 °C prior the experimentation.

Ash leaching experiments were conducted at a fixed concentration of solid phase (5.0 g L^{-1}) in sterile, pre-cleaned polypropylene bottles, in triplicates. The bottles were gently stirred on a ping-pong shaker (100 rpm) at 20 ± 0.5 °C in darkness. One series of experiments was conducted with Milli-Q distilled water and another with natural organic-rich lake water (DOC of 40 mg L^{-1}). The choice of these two media was to model the two main scenarios of vegetation ash behavior in natural systems after massive fire events: 1) leaching by rainwater and 2) transfer of ash particles to

organic-rich surface waters (notably to soil depressions and small thaw ponds).

After 1, 5, 10, 30, 100, 300, 1440, 3000 and 10,020 min of reaction, the replicate bottles were removed from the shaker and the contents of each bottle were entirely used for chemical analyses. Aqueous suspensions were filtered immediately after sampling using a sterile syringe and a disposable, single-used 0.45 μm Millipore filter unit.

2.3. Chemical analyses

The pH and electrical conductivity were measured in unfiltered waters immediately after sampling using Hanna and WTW portable instruments. Dissolved organic carbon (DOC) and major and trace elements were measured in 0.45-μm filtered samples after their storage of 5 to 7 days in the refrigerator. The major anion concentrations (Cl^- and SO_4^{2-}) were analyzed by ion chromatography (Dionex 2000i) with an uncertainty of 2 %. The international standards ION, PERADE, and RAIN were used for validation of analyses. DOC and dissolved inorganic carbon (DIC) were determined by a Shimadzu TOC-VSCN Analyzer with an uncertainty of 3 % and a detection limit of 0.1 mg L^{-1}. Specific UV absorbance (SUVA) was measured as absorbance at 254 nm normalized for DOC concentration in L mg^{-1} m^{-1}. Major cations (Ca, Mg, Na, K), Si and ~40 trace elements were determined with an Agilent iCap Triple Quad (TQ) ICP MS using both Ar and He modes to diminish interferences. About 3 μg L^{-1} of In and Re were added as internal standards along with 3 various external standards. Detection limits of TE were determined as 3× the blank concentration. The typical uncertainty for elemental concentration measurements ranged from 5 to 10 % at 1–1000 μg L^{-1} and 10–20 % at 0.001–0.1 μg L^{-1}. The Milli-Q field blanks were collected and processed to monitor for any potential contamination introduced by our sampling and handling procedures. The SLRS-6 (Riverine Water Reference Material for Trace Metals certified by the National Research Council of Canada) was used to check the accuracy and reproducibility of analyses (Heimburger et al., 2013). Only those elements that exhibited good agreement between replicated measurements of SLRS-6 and the certified values (relative difference <15 %) are reported in this study.

Chemical analysis of ash constituents was performed using an X-ray Fluorescence spectrometer (X Bruker S2), via fusing with Li borate at 1200 °C (XRfuse6, Bruker) and using a set of sediment and rock standards to quantify major elements (i.e., Na, Mg, Al, Si, P, S, K, Ca, Mn, Ti, Fe) with an average uncertainty of 1 %. Concentrations of these elements were in agreement with certified values of geostandards and were within 10 %. Morphology and chemical composition of ash particles were also examined via SEM (Scanning Electron Microscopy) using a Tescan Vega 4 LMU electron microscope equipped with an EDX (energy-dispersive X-ray) detector of SDD Bruker Quantax 30mm^2.

2.4. Statistical tests

Experimental parameters which included pH, temperature, and all measured major and trace element concentrations were analyzed with best fit functions. The best fit functions were based on the Pearson correlation and a parametric ANOVA (Analysis of Variance) on samples where the Shapiro-Wilk test yielded the normality of the data and the Barlett test demonstrated homogeneity of variance. Regressions and power functions were used to examine the relationships between pH, DOC, and major and trace element concentrations as a function of leaching time. The criterion for significant correlation between the chemical parameters was $p < 0.05$. If the ANOVA was significant at $p < 0.05$, a parametric Student *t*-test and Tukey test were used given that data were normally distributed. A lower probability ($p < 0.05$) indicated that the overall differences in concentration – time trend are important and statistically significant compared to internal variations between replicates. The pairwise trace element correlations (Cl, SO_4, Si, P, K, Al, Fe, Ca and DIC as major leachable constituents of ash material) in the filtrates over the course of incubation experiments were tested using Pearson correlation (SigmaPlot version 11.0, Systat Software, Inc.) for all aqueous solutions and separately for peat, lichen and moss ash at $p < 0.05$. The weight loss of ash in the course of experiment was calculated based on the sum of inorganic solutes Ca, Mg, Na, K, Si, P, Al, Cl, DIC and SO_4, normalized to oxides, in order to monitor the degree of solid phase dissolution. The apparent bulk rates of element removal from ash (mass-normalized elementary yields) were calculated for the first 50 h of reaction and for the remaining period of exposure (50–167 h). The reason of choosing 50 h as a threshold time for rate calculation is that the majority (>80–90 %) of ash constituents were leached during first 2 days of experiment.

3. Results

3.1. Chemical and mineralogical nature of ash

Ash content of the studied organic substrates followed the order: lichen (0.75 wt%) < moss (1.75 %) < peat (2.5 %). The SEM examination of lichen ash demonstrated that it contains a sizable amount of sand (quartz) grains, isomeric particles of black carbon, and other particles of irregular shape containing K, P, Ca, Si, Mg, Al and Fe (**Fig. S1 A**). Results of semi-quantitative SEM-EDX examination of lichen ash particles were consistent with the data of total chemical analysis performed by XRF and demonstrated a high proportion of Si (88 % SiO_2), followed by Al (3.2 % Al_2O_3), K (2.0 % K_2O), Ca (1.7 % CaO) and Fe (1.1 % Fe_2O_3), **Table S1**. Moss ash demonstrated the presence of clearly identifiable phytoliths and diatom frustules, black spheres of amorphous Si 5 to 10 μm in diameter, and various irregular particles with typical elements (other than C and O) detected by EDX being Si, Al, K, Fe, Ca, Mg, Na, P (**Fig. S1 B**). Total chemical analysis of moss ash demonstrated, in addition to Si, high concentrations of S (15.3 % SO_3), K (1.5 % K_2O), Ca (14.7 % CaO), Mg (9.7 % MgO), P (6.4 % P_2O_5), Na (3.6 % Na_2O) and Fe (2.5 % Fe_2O_3). Peat ash contained vegetation debris and phytoliths, with high concentrations of Si, Fe, Al, Ca and S (**Fig. S1 C**). Accordingly, total chemical analysis of peat ash showed dominance of Si (43 % SiO_2), followed by Al (11.4 % Al_2O_3), Fe (11.0 % Fe_2O_3), Ca (10.8 % CaO) and S (7.8 % SO_3). XRD analysis of lichen and peat ash demonstrated only quartz peaks whereas moss ash yielded these same peaks and those showing some presence of calcite and dolomite (**Fig. S2**).

3.2. Element concentrations and yields during ash dissolution

A foremost important experimental result is the drastic difference in the aqueous reactivity of vegetation ashes. Among the three substrates, moss ash was by far (a factor of 2 to 10) more reactive because it yielded the largest changes in solute concentration over first 2 days of reaction time (Fig. 1 and Table 1). Thus, moss ash produced sharper change in fluid pH (10 over the first 100 min of reaction, gradually decreasing to 8 after several days of exposure) regardless of the nature of the liquid substrate (Milli-Q water or lake water), as illustrated in Fig. 1. In contrast, peat and lichen ash only slightly modified the pH of the fluid, which decreased from 6 to 5 over the experiments with both Milli-Q and lake water. Similarly, moss ash released a much larger amount of soluble salts into the fluid compared to the other two substrates; the water Electric Conductivity in moss ash experiments ranged from 400 to 600 μS cm^{-1} compared to 100 to 200 μS cm^{-1} for peat and lichen ash. Chloride exhibited steady release in both aqueous solutions with maximal effects observed in moss; sulfate concentration, also maximal (2 to 3 times higher) in moss compared to other substrates, remained rather constant after an initial abrupt increase at the very start of experiment (Fig. 1).

Another experimental result is the very fast change in aqueous solution composition, for both Milli-Q water and lake water runs, so that the concentrations of these constituents were orders of magnitude higher than those of the starting solutions, and this occurred after the first minute of reaction, as can be seen in Figs. 1, 2 and 3. We also noted that the total weight loss (in % of the initial mass of solid) became constant after the first hours of reaction following the order: peat (<1.5 %) ≤ lichen (1.5–2 %) < moss (3 %). The

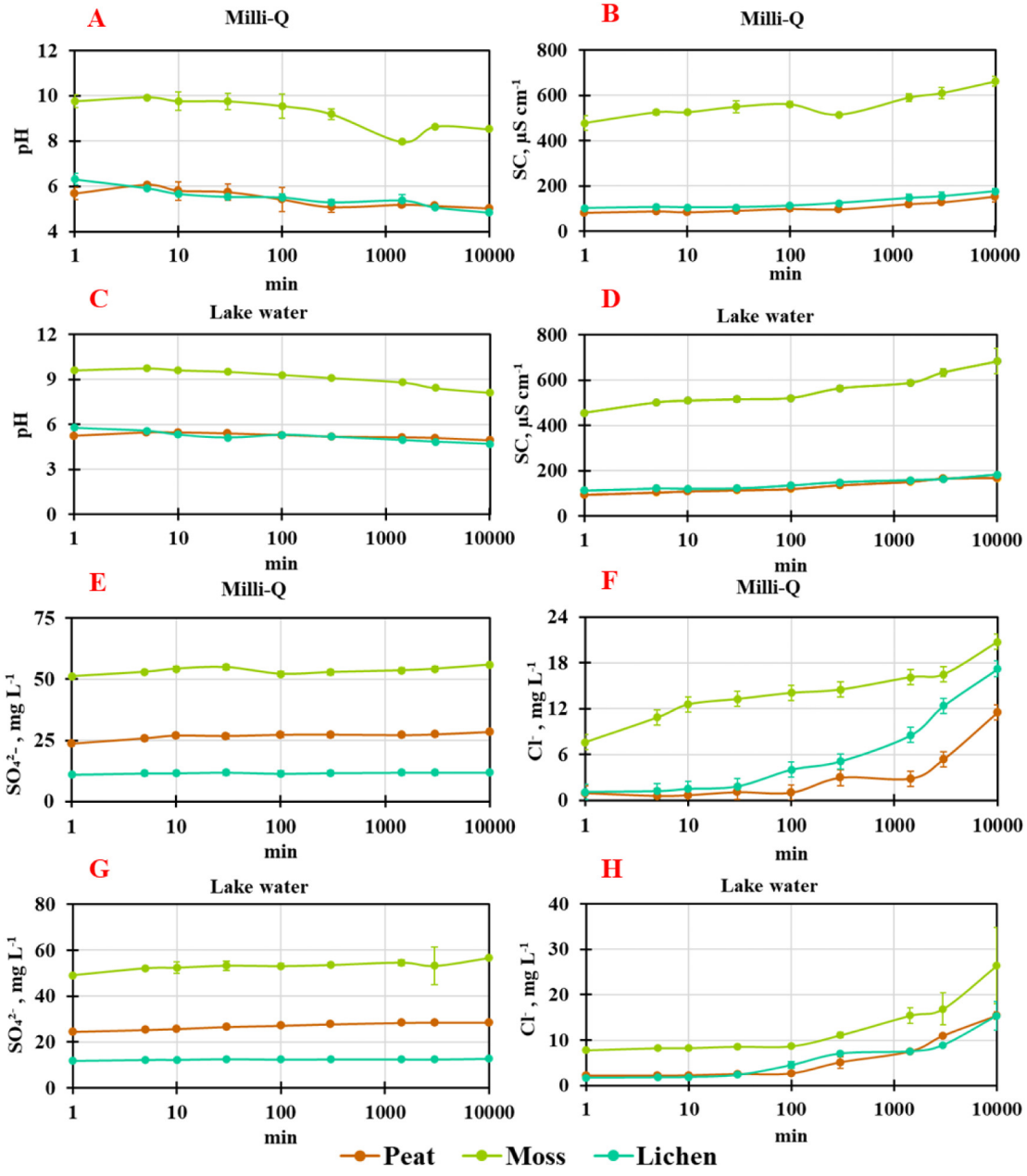

Fig. 1. The pH and SO_4^{2-} (left panels, A, C, E, G) and Specific Conductivity and Cl^- (right panels, B, D, F, H) evolution as a function of elapsed time in ash dissolution experiments in the Milli-Q water and lake water. The symbols are mean values of three independent experiments, whereas the error bars represent s.d. uncertainty of triplicates (unless not shown because they are within the symbol size).

80 to 90 % of elemental release over first 10 min was observed for major elements (SO_4, Si, P, Mg, K and Ca), Al, Fe, micronutrients (V, Cr, Mn, Cu, Zn, Se, Sr, Rb and Mo), trivalent and tetravalent hydrolysates, trace oxyanions and heavy metals.

The temporal pattern of elemental release from three ash samples was generally similar between DOC-rich lake water and distilled water, which allowed generalizing the element concentration evolution among different solid substrates and aqueous solutions. According to the temporal evolution of concentration during experiments, 2 main groups of major and trace elements were identified (**Table S2**). The 1st group includes major anions such as Cl, SO_4 and DIC, cations such as Na, Mg, Ca and K, macro and micronutrients (Si, P, Co, Mo, Rb and Se) and other trace elements (Ti, Cr, As, Sb, Zr, Y, Cs, Ba, Tl, Th) that steadily increased in concentration over the course of exposure or kept essentially constant [after an abrupt, almost instantaneous increase over the first minute of reaction]. Examples of labile elements in this group (Si, P, Mn, Co, As, Mo, Sb, Rb) are illustrated in Fig. 2. Note that this 1st group can be subdivided into two main chemical behavioral types: 1) *Cl-type elements* (Cl, B, Mg, Si, P, Ti, Mn, Co, As, Zr, Mo, Sb and Th) gradually increasing their concentration with time and 2) *SO_4-type elements* (Na, K, Ca, Cr, Mn, Fe, Se, Rb, Sr, Cs and Ba) exhibiting high concentration after the first minute of sampling with a rather constant pattern afterwards.

The 2nd group is formed by those elements exhibiting a systematic decrease in pH value and a decrease in concentrations of Cu, Zn, Cd, Y, LREE and U after the beginning of leaching experiment. In the DOC-rich lake water, DIC and DOC decreased their concentration as illustrated in Fig. 3 (for DOC, Cu, Zn and Cd) and **Fig. S3** for V, Y, La and U. In contrast to DOC (Fig. 3**G**), the SUVA of the lake water systematically increased in the presence of all three ashes (Fig. 3**H**). Some elements demonstrated non-systematic variation over time when reacting with moss and lichen ash, with a local maximum or both maximum and minimum (Cu, V, heavy REEs and Th).

Table 1
Element yield (mean ± s.d.) from peat, moss and lichen ash to aqueous solution (averaged for Milli-Q water and organic-rich lake water) over 167 h of reaction.

	Peat ash	Moss ash	Lichen ash
	mg/g^{-1}		
DIC	0.20 ± 0.20	4.71 ± 4.90	0.24 ± 0.25
DOC	1.68 ± 1.68	4.00 ± 4.22	2.41 ± 2.61
SO_4^{2-}	5.69 ± 0.10	11.26 ± 0.11	2.48 ± 0.12
Cl-	2.69 ± 0.58	4.71 ± 1.10	3.26 ± 0.41
	$\mu g/g^{-1}$		
B	2.75 ± 0.19	21.3 ± 0.29	10.6 ± 0.37
Na	274.8 ± 79	1575 ± 124	315 ± 70.5
Mg	614 ± 51	2330 ± 86	96.3 ± 15.4
Al	8.52 ± 3.0	66.4 ± 11.4	77.4 ± 33.1
Si	115 ± 19.7	490 ± 39	718 ± 41
P	599 ± 93	814 ± 59	3878 ± 206
K	2429 ± 502	20,865 ± 2280	7869 ± 1450
Ca	1663 ± 112	1566 ± 86	95.6 ± 22.9
Ti	0.10 ± 0.049	0.21 ± 0.11	3.77 ± 1.73
V	0.13 ± 0.013	2.35 ± 0.18	0.15 ± 0.038
Cr	0.05 ± 0.035	0.44 ± 0.0069	0.46 ± 0.15
Mn	0.82 ± 0.11	27.9 ± 4.6	2.91 ± 0.49
Fe	2.81 ± 1.69	3.52 ± 3.04	62.3 ± 28.8
Co	0.044 ± 0.0051	0.22 ± 0.049	0.051 ± 0.010
Ni	0.059 ± 0.0080	1.21 ± 0.29	0.21 ± 0.11
Cu	0.040 ± 0.0087	0.19 ± 0.031	0.22 ± 0.11
Zn	1.46 ± 0.14	0.82 ± 0.47	2.74 ± 0.66
As	0.26 ± 0.022	0.94 ± 0.014	0.89 ± 0.073
Se	0.10 ± 0.0087	0.44 ± 0.027	0.11 ± 0.010
Rb	0.69 ± 0.066	63.0 ± 2.1	18.0 ± 0.81
Sr	14.3 ± 0.53	2.71 ± 0.08	0.28 ± 0.067
Y	0.0023 ± 0.00042	0.0023 ± 0.0010	0.010 ± 0.0063
Zr	0.0082 ± 0.0037	0.0087 ± 0.0047	0.16 ± 0.056
Mo	0.094 ± 0.014	0.55 ± 0.035	0.18 ± 0.010
Cd	0.0040 ± 0.00038	0.0030 ± 0.0014	0.0069 ± 0.0026
Sb	0.063 ± 0.0037	0.70 ± 0.048	0.32 ± 0.016
Cs	0.021 ± 0.0022	0.96 ± 0.047	0.24 ± 0.014
Ba	6.17 ± 0.39	2.38 ± 0.094	0.38 ± 0.085
La	0.0012 ± 0.00025	0.0026 ± 0.0018	0.015 ± 0.0077
Ce	0.0021 ± 0.00031	0.0039 ± 0.0039	0.028 ± 0.012
Pr	0.00027 ± 0.000034	0.00041 ± 0.00041	0.0035 ± 0.0017
Nd	0.0011 ± 0.00018	0.0018 ± 0.0014	0.013 ± 0.0068
Sm	0.00041 ± 0.000087	0.0026 ± 0.0037	0.0033 ± 0.0018
Eu	0.00077 ± 0.000037	0.00035 ± 0.000075	0.00062 ± 0.00031
Gd	0.00025 ± 0.000080	0.00030 ± 0.00027	0.0023 ± 0.0013
Tb	0.000032 ± 0.0000081	0.000044 ± 0.000031	0.00032 ± 0.00017
Dy	0.00017 ± 0.000024	0.00024 ± 0.00018	0.0018 ± 0.00090
Ho	0.000036 ± 0.0000044	0.000048 ± 0.000032	0.00036 ± 0.00020
Er	0.00011 ± 0.000023	0.00014 ± 0.000091	0.0010 ± 0.00058
Tm	0.000019 ± 0.0000037	0.000020 ± 0.000013	0.00014 ± 0.000082
Yb	0.00012 ± 0.000021	0.00013 ± 0.000087	0.00088 ± 0.00053
Lu	0.000020 ± 0.0000036	0.000022 ± 0.000015	0.00013 ± 0.000078
W	0.0026 ± 0.0017	0.23 ± 0.023	0.10 ± 0.014
Tl	0.0056 ± 0.0047	0.0071 ± 0.0044	0.0047 ± 0.00027
Pb	0.015 ± 0.0036	0.046 ± 0.028	0.27 ± 0.094
Bi	0.0013 ± 0.00069	0.0016 ± 0.00060	0.010 ± 0.0047
Th	0.00076 ± 0.00091	0.0011 ± 0.00081	0.035 ± 0.0032
U	0.00013 ± 0.000010	0.013 ± 0.0022	0.0012 ± 0.00070

Both elemental groups identified were confirmed by pairwise (Pearson) correlations which simultaneously tested both the aqueous media and the three ashes, as well as individually, for each ash of each material (**Table S3**). Considering all the solid substrates together, in the leachates, labile elements (B, Na, V, Se, Mo, Rb, Cs, Sb and U) strongly correlated with K ($R_P \geq 0.90$; $p < 0.01$) whereas immobile elements (Ti, Zr, Y and REEs) correlated with Fe ($R_P \geq 0.80$; $p < 0.05$). This has also been observed individually for moss and peat ash leachate. In the peat ash leachate, Al strongly correlated with low solubility Ti, Cr, Fe, Zr and REEs ($R_P > 0.91$; $p < 0.01$) indicating a concomitant release of these elements from (refractory) silicate minerals of peat.

The yields (mass of element released into aqueous solution over a given amount of time and normalized to initial mass of ash) for the first 2 days (0–50 h) and subsequent 7 days (50–167 h) of leaching in the Milli-Q and lake water for three ash materials (Table 1) are illustrated for some elements in Fig. 4. Exempting Si and Cl, the main release of all elements, including DOC, occurred over the first 2 days for all ashes with <20 % of release occurring between subsequent 50 and 167 h of reaction. Phosphorus from lichen ash and Mg from moss ash demonstrated 20–30 % release during the second stage of reaction. DIC was also sizably (50 %) released during the second stage from moss ash. There was no sizable difference in element release patterns between distilled water and organic-rich lake water (Fig. 4). Release of the largest number of major and trace elements was dominated by moss followed by lichen and peat ash (Table 1). These included DOC and DIC, labile macro- and micro-nutrients (B, Cl, SO_4, Na, Mg, K, Mn, V, Zn, Se, Rb, As, Mo, Sb, Cs, W and U) and some trace metals (Al, Cr, Cu, Co, Ni and Cd). The 2nd group of elements, whose yield was dominated by lichen rather than moss and peat, included two major nutrients (Si, P) and a number of low mobility elements such as Fe, Ti, Y, Zr, REEs, Pb and Th. Lastly, the yield of alkaline-earth elements was highest in the peat ash followed by moss and lichen ash. The order of release from peat: moss: lichen was 17:16:1, 50:10:1, and 16:6:1 for Ca, Sr, and Ba, respectively.

3.3. Tundra fire impact on rivers and lakes

The experimental results on short-term aqueous reactivity of the three organic substrates dominating the palsa peatlands in western Siberia (moss, lichen and upper peat layer) allow first-order quantification of tundra fire impact on element mobilization from burnt surface to the hydrological network. Considering the proportion of ash in peat, lichen and moss (2.5 ± 0.5, 0.8 ± 0.1 and 1.8 ± 0.7 wt%, respectively), the average elemental content of water-soluble (leachable) elements in organic matter ash can be calculated as the average yields in Milli-Q water and lake water (Table S4). The fresh (dry) organic mass – normalized element yield preserved the same order 'moss > lichen > peat' for most macro and micro-nutrients. Considering the total moss and lichen biomass coverage of typical permafrost palsa peatbogs is 1:1, the typical lateral stock of moss and lichen in the northern part of western Siberia is 290 and 245 $g_{d.w.}\ m^{-2}$, respectively (Kosykh et al., 2008). For this region, with typical peat density of 0.09 kg cm^{-3}, the upper 0–10 cm peat mass stock is 9000 $g_{d.w.}\ m^{-2}$ (Novikov et al., 2009).

The frozen peatbog (palsa) surface area that is subjected to annual burning in the north of western Siberia has not been quantified yet but can be approximated as 40 % of the total surface per 60-year period (of which tundra and palsa together account for ¾ of total land area according to Sizov et al. (2021)). Therefore, the northern palsa peatbogs of WSL can be entirely burned each 56 years, which is in agreement with our unpublished results on radiogenic C dating, as well as with the latest estimates for the forest tundra and northern taiga of Central Siberia (Novenko et al., 2022; Dvornikov et al., 2022). Note that the average fire rotation time in Eastern and Central Siberian taiga and tundra was recently estimated at 126 years (Talucci et al., 2022), whereas more conservative estimation suggests entire palsa burning each 150 years (Sizov et al., 2021; Novenko et al., 2022). In order to quantify possible release of elements from burned vegetation and peat, we will consider a flat watershed divide near the Khanymey Research Station, containing 40 % of lakes, 28 % of palsa peatbogs, 8 % of forest and 24 % of wet depressions and fens (Novikov et al., 2009). Assuming a fire return frequency of 56 years, the wildfire in this region can burn annually 1450, 1225 and 45,000 kg km^{-2} of sphagnum, lichen and 0–10 cm peat, respectively. Note that in this scenario, we ignore burning of dwarf shrubs and grasses in the palsa and organic litter and forest floor in the forested regions.

These aerial stocks of moss, lichen and upper peat layers, combined with water-soluble element concentrations in vegetation and peat ash (Table 1, **Table S4**) allow for quantification of the water-soluble yield of element from the watersheds of permafrost peatbogs. For this, assume that the ash produced during tundra burning is entirely mobilized into hydrological network (**Table S5**). In such a scenario, we test the maximal impact of tundra wildfire on element transfer from the soil to the aquatic systems. In this table, we separately present the water-labile stock of element in peat,

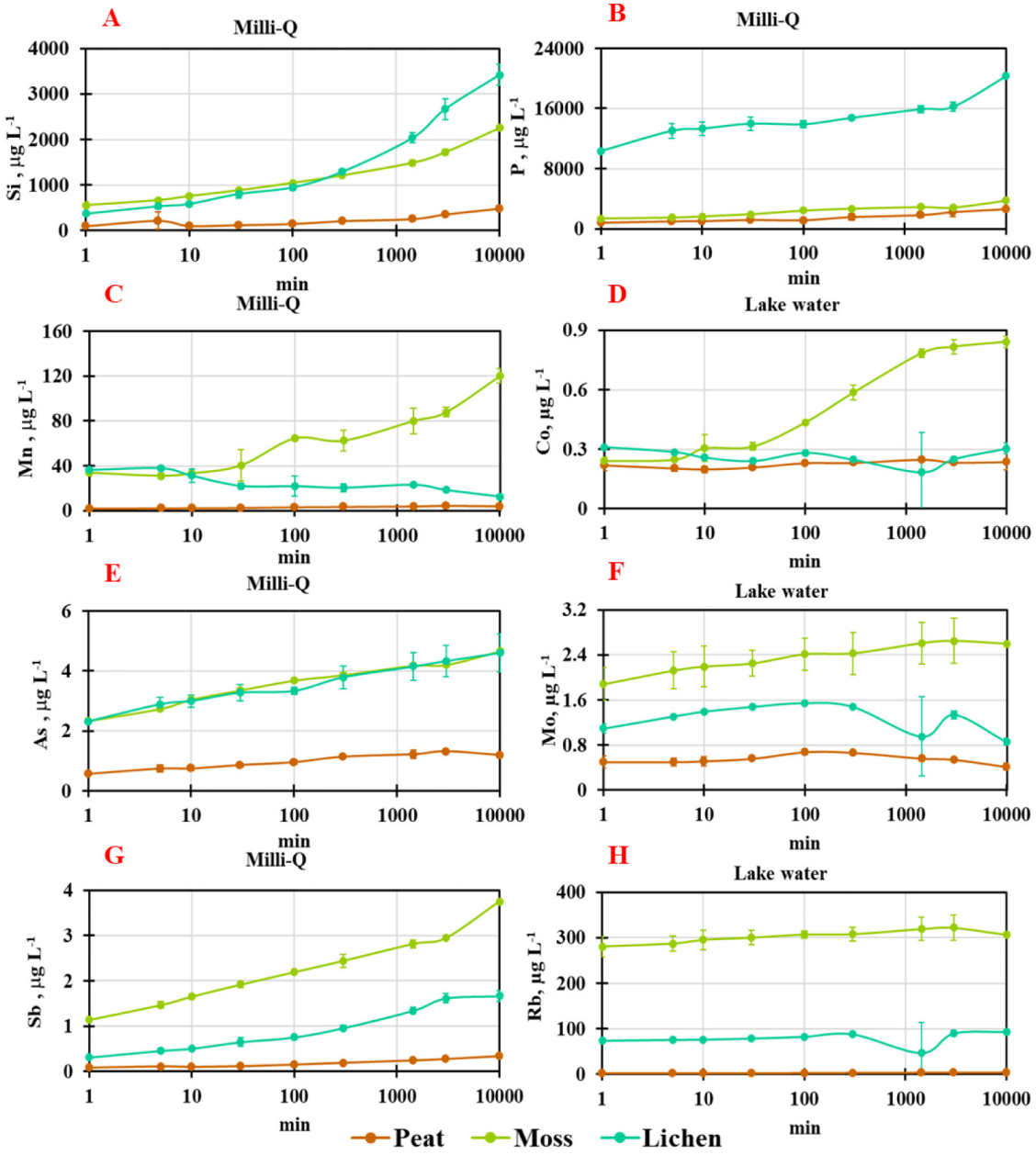

Fig. 2. Example of 1st group element evolution in the course of ash leaching in MilliQ water (left panels) and lake water (right panels): Si (A), P (B), Mn (C), Co (D), As (E), Mo (F), Sb (G) and Rb (H). The symbols are mean values of three independent experiments, whereas the error bars represent s.d. uncertainty of triplicates (unless not shown because they are within the symbol size).

moss and lichen ash as well as integral yield of elements from burning of moss, lichen and upper 0–10 cm peat layer. We further assume that all palsa surfaces are burned each 56 years. These possible annual ash-originated element yields can be compared with actual annual yields of major and trace elements by small and medium sized rivers draining through palsa peatbogs of western Siberia; these have been assessed via hydrochemical and hydrological analyses of >30 rivers across the seasons in this region (Pokrovsky et al., 2020). For this investigation, we calculated a ratio of annual element leaching from burned vegetation to annual hydrochemical yields (Fig. 5). Overall, the impact of palsa fire on element export from the fire-affected watershed by rivers is negligible and does not exceed 0.1–0.2 % of annual riverine yield for most major and trace elements. Only the riverine yield of Mo, Rb and Sb could be affected by tundra fire at about 0.5–1 % and that of K, SO_4 and Cs at 2–2.5 %.

Another mass balance calculation was performed to assess the possible impact of tundra fire on the hydrochemistry of thermokarst lakes that are highly abundant in permafrost peatlands. For this, we considered two extreme scenarios of the lake coverage in the territory subjected to wildfire: 40 % for the Khanymey Research station test site described above and 4 % which represents the minimal limnicity of a much larger (i.e., 1 million km^2) permafrost-affected part of the WSL (Polishchuk et al., 2018). The average lake depth in the permafrost palsa peatlands was assumed to be 1 m (Manasypov et al., 2020). We further assumed that all ash produced by tundra burning will be delivered to adjacent lakes via surface or suprapermafrost flow, which represents maximal possible impact of a wildfire event. The range of major and trace element concentrations in the continuous and discontinuous permafrost zones of the WSL is based on seasonal analysis of >70 lakes across a permafrost gradient (Manasypov et al., 2020). These mass-balance calculations demonstrate

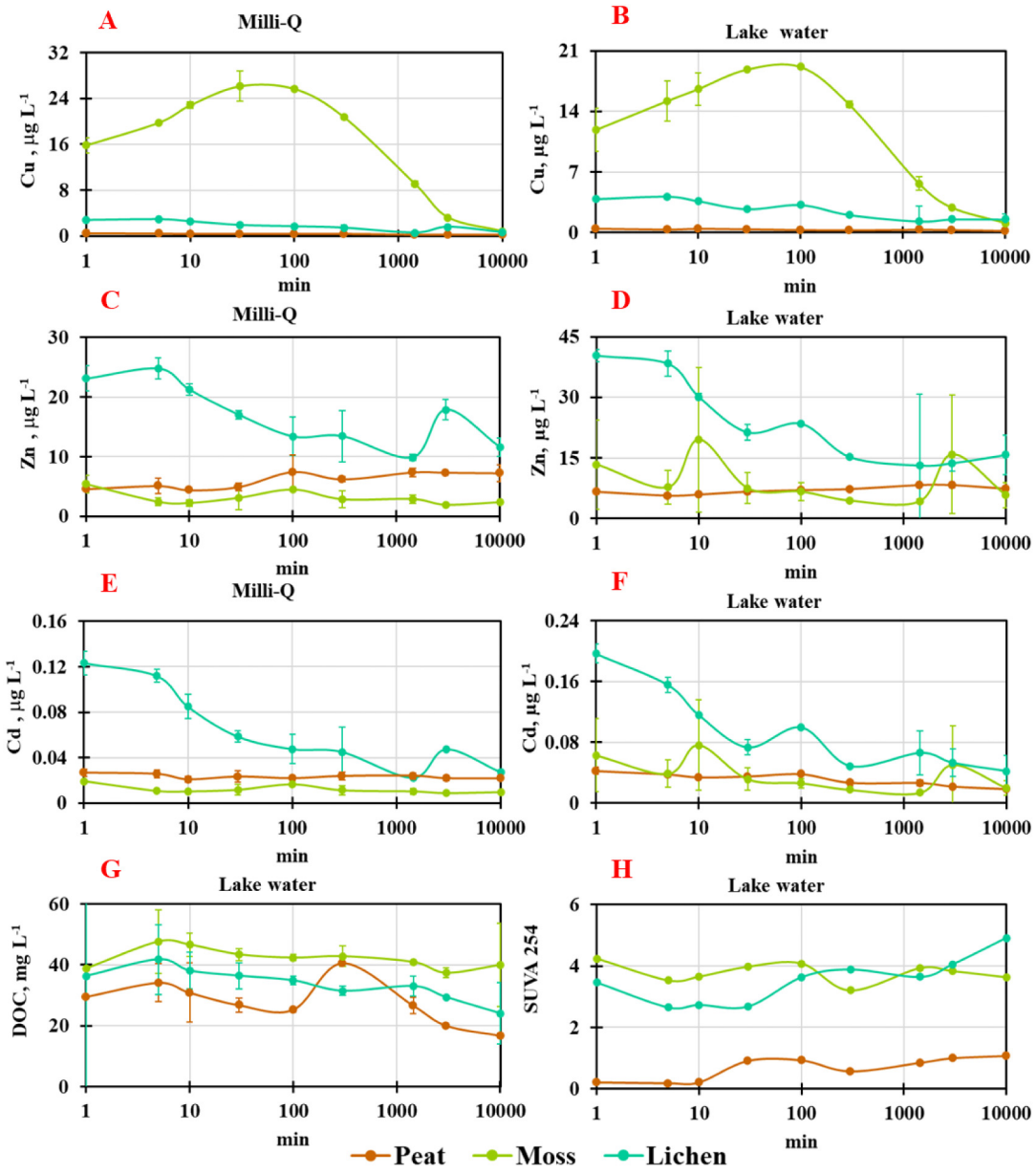

Fig. 3. Example of 2nd group element evolution (decreasing concentration with time) in the course of ash leaching in Milli-Q water and lake water: Cu, Zn, Cd, DOC and $SUVA_{254}$. The symbols are mean values of three independent experiments, whereas the error bars represent s.d. uncertainty of triplicates (unless not shown because they are within the symbol size).

that the concentration of overwhelming majority of dissolved elements present in the thermokarst lake water column will be negligibly (<1–2 %) impacted by ash product delivery even in the case of minimal possible limnicity (4 %) of the territory. One exception is Ca, whose concentrations in thermokarst lakes (range 0.2–1.2 mg L^{-1}, Manasypov et al., 2020) can be non-negligibly affected by ash leaching in a scenario of low limnicity (addition of 0.18 mg L^{-1}). Finally, only phosphorus originated from ash dissolution (addition of 2 and 20 µg L^{-1} for watersheds having 40 and 4 % of lake coverage, respectively) can sizably modify the current P_{tot} concentration in WSL lakes (1 to 3 µg L^{-1}).

Note that the mass-balance calculations presented above have to be considered with caution because we averaged a unique event of total palsa burning (28 % of the territory) to the total duration of fire return frequency (56 years). A single-year effect of moss, lichen and upper peat burning on element export by rivers and lake hydrochemical composition might be drastically (up to 56 times) higher. In such a case, the delivery of ash leaching product can at least double most element fluxes and pools in aquatic systems for that particular year.

4. Discussion

4.1. Nature of ash from moss, peat and lichen

Numerous works have documented the extremely high reactivity of ash formed on the surface of the soil after a fire and its particular enrichment in essential nutrients like N, S, P and K (Koyama et al., 2010; Harden et al., 2004; Neff et al., 2005; Pereira et al., 2012). In contrast to the vast amount of literature devoted to physico-chemical properties and reactivity of wood and grass ash (Fang and Jia, 2012), the information on chemistry and mineralogy of peat, moss and lichen ash remains rather limited. In peat ash, the dominant Si compounds are known to be quartz with occasional amounts of K and Na feldspar; alternatively, clay minerals in peat provide high Al and

Fe contents (Steenari et al., 1999). Calcium is known to occur as an oxide, carbonate or sulfate and Mg and P are not usually identified in crystalline form (Steenari et al., 1999). The results of the present study generally agree with the bulk of available information on ash chemical composition and allow for understanding the relative difference in the leachability of different elements. Thus, the total chemical composition of different ashes (**Table S1**) followed an order which is similar to the order of element leachability observed in the experiments such as 'moss' > 'peat' > 'lichen' for Na, Mg, Si, P, Mn and 'peat' > 'moss' ≥ 'lichen' for Al and Fe. The moss ash released a factor of 2 to 10 higher amount of alkalis (Na, K, Rb, Cs) and nutrients (P, Mn) compared to other ashes because it contained the highest concentrations of these elements in the solid phase. In contrast, Si was mostly leachable from lichen ash (2 and 6 times higher than from moss and peat, respectively, Table 1), where it was concentrated in the form of amorphous silicate material and quartz grains. Although peat ash contained two times more total Si than the moss ash, the later exhibited about four times higher leachable Si compared to peat ash (Fig. 4). This is presumably due to the abundant pool of reactive silica in the form of phytoliths and diatom frustules (**Fig. S1**).

Note that, although the resolution of XRD analysis (1–2 % (*w*/w)) generally does not allow detecting crystalline phases in ash (i.e., Steenari et al., 1999), among all three studied substrates, only the moss ash demonstrated some peaks of calcite and dolomite (**Fig. S2**). We believe that the presence of these highly soluble carbonate minerals containing various trace components is responsible for the highest yield of Mn, Co, V, Ni, Cu and other divalent metals which could be associated with these minerals in the moss

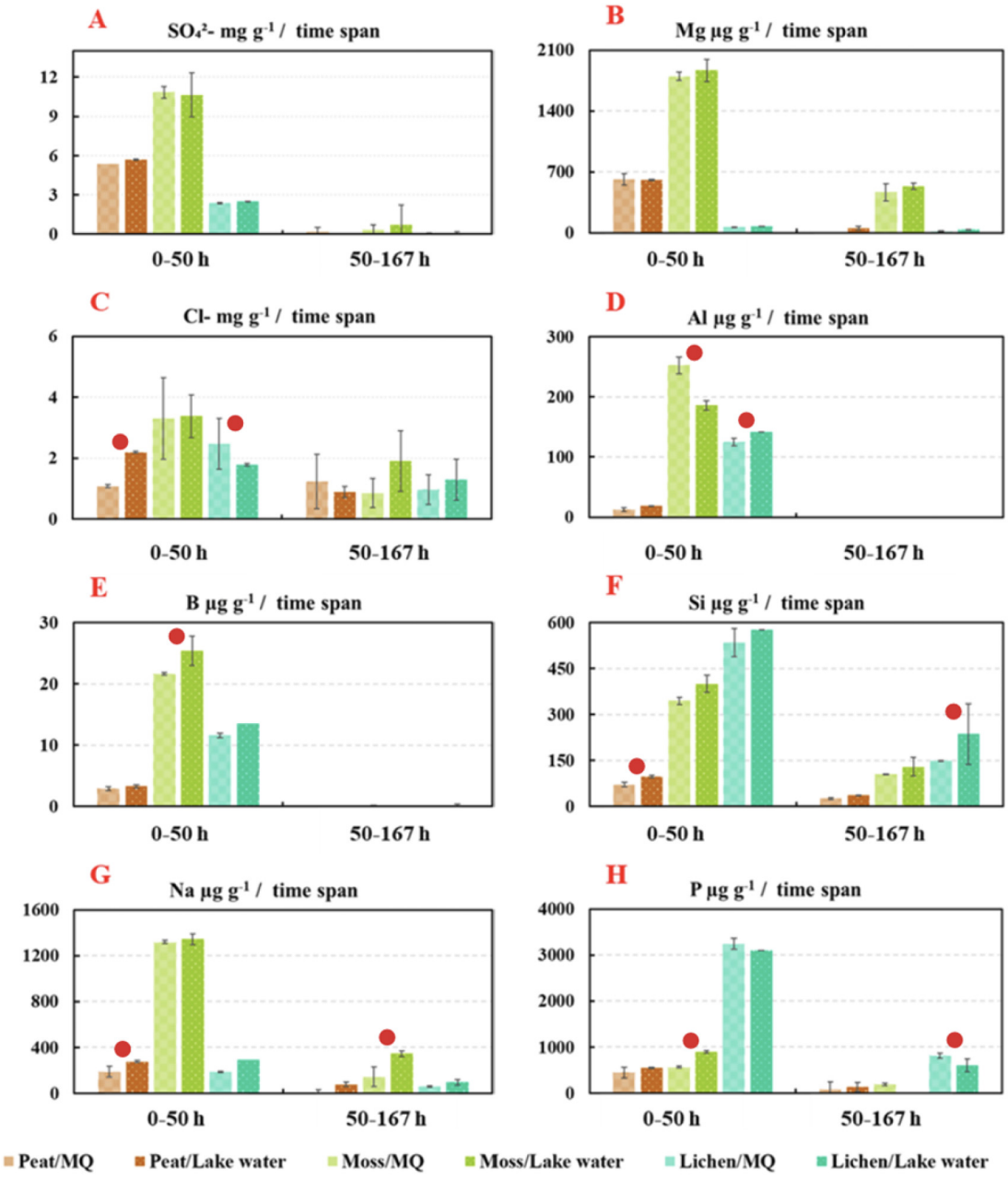

Fig. 4. Elementary yields (normalized to the mass of ash) over the first 2 days and subsequent 7 days of reaction with peat, moss and lichen ash. The columns and error bars represent the mean values and s.d. of three independent experiments for each solid and liquid substrate. The red circle indicates significant differences (at $p < 0.05$) between Milli-Q and lake water.

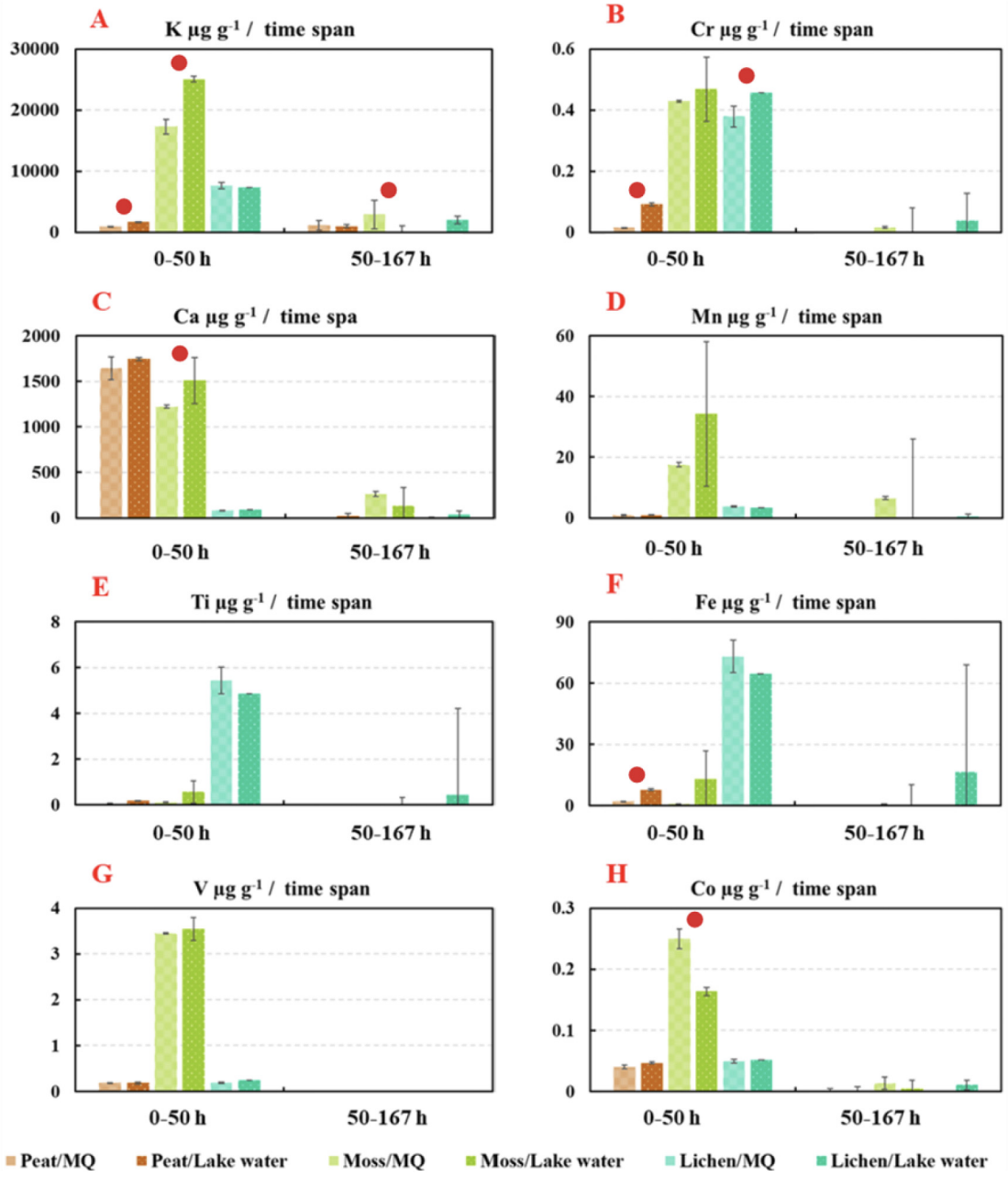

Fig. 4 (*continued*).

ash. Further physico-chemical studies of ash reactivity with high resolution spatial examination of both initial solid phases and the reaction products, including laser ablation ICP-MS and Transmission Electron Microscopy are needed to reveal chemical and mineralogical controls on element leachability from ash to aqueous solution.

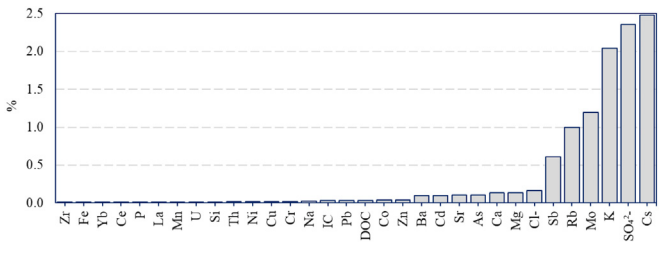

Fig. 5. Histogram of ratio (in %) of annual element leaching from burned vegetation in the palsa watershed of permafrost peatlands assessed in this study (**Table S5**) to annual elementary yield by small and medium size rivers in permafrost impacted portions of the WSL (from Pokrovsky et al., 2020).

4.2. Mechanisms of element leaching from ash

In this section, we discuss the impact of aqueous substrate and mineral source in the solid phase on patterns of element leaching from ash. Most elements constituting the ash material produced after wildfires are present in a water-soluble state (Pereira et al., 2012) and exhibit extremely high mobility in soils (Christensen, 1973; Grier, 1975; Kaufmann et al., 1993). Previous field mesocosm experiments in thermokarst lakes with various organic and inorganic substrates demonstrated that ash is extremely reactive in natural waters, and >90 % of its elemental stock is released over the first 10 h (Manasypov et al., 2017). High-resolution laboratory experiments of the present study demonstrate even faster release of ash constituents with the majority (>80 %) of labile elements mobilized from the solid phase over the first 10 min. Unfortunately, the resolution of our sampling

and filtration did not allow testing the kinetics of dissolution over a shorter time period. Furthermore, given that such fast rates of ash dissolution likely reflect diffusional versus surface reaction control (i.e., Schott et al., 2009), alternative techniques of measuring ash reactivity (column-through experiments, rotating disk technique, etc.) are needed to quantify rate constants.

Only a few elements demonstrated gradual change in concentration. This could be linked to mineral dissolution/precipitation controlled by a gradual pH change. This was especially pronounced for moss ash, whose pH decreased up to 2 units over the course of experiment. We therefore hypothesize that labile elements which gradually increased in concentration over time (Cl, DIC, B, Mg, Si, P, Mn, Co, Mo, As and Sb) were incorporated into or adsorbed on the surface of soluble (amorphous) salts such as carbonates, phosphates, oxides or silicates of Na, K and Ca. The dissolution rate and solubility of these sparingly soluble salts is known to increase (e.g., Schott et al., 2009) with a decrease in pH (from 10 to 8 for moss ash and from 6 to 5 for peat and lichen ash). Therefore, such a pH decrease in the course of present experiments could progressively release the aforementioned elements to the aqueous solution.

Note that an enhanced mobility of oxy-anions at high pH was created by moss ash dissolution as this solid substrate demonstrated the highest yield of Mo, Se, Sb, W and U. This observation can be explained by a desorption of these oxyanions from moss ash mineral particles. Among these elements is dissolved $U^{(VI)}$ most likely present in the form of uranyl-carbonate or hydroxyl complexes. In contrast, the decrease of Al concentration after 100 min of reaction observed in moss ash experiments in lake water and Milli-Q water could be due to the solubility threshold of amorphous Al hydroxide starting to precipitate from aqueous solution below pH 9.

Another group of labile elements (i.e., SO_4, Na, K, Ca, Cr, Se, Rb, Sr, Cs and Ba) exhibited high concentrations after first minute of ash-aqueous solution reaction followed by a rather constant pattern afterwards. We believe that fast dissolution of sparingly soluble sulfates of alkaline-earth and alkaline metals can be responsible for this behavior. A sizable correlation of highly mobile B, Na, V, Se, Rb, Mo, Cs, Sb with K (and to a lesser degree SO_4; **Table S3**) in leachates from all three ashes may indicate presence of these elements in the form of K hydroxide and sulfate. It is also possible that ash material, formed after biomass burning, was composed of multilayer amorphous/semi-amorphous solid phases of varying chemical composition and reactivity so that progressive surface layer dissolution could expose the interior of the particle to leaching. This could produce a stepwise element concentration pattern. For example, progressive removal of an external Ca silicate, sulfate or phosphate layer at the beginning of reaction exposed a more soluble inner layer containing Na and Mg chloride. To further examine this possibility, high-resolution future transmission electron microscopy coupled with elemental analysis has to be performed on both initial phases and reaction products.

The last group of elements was represented by those showing a systematic decrease in concentration over time, detectable after the first minute of reaction: pH value, Cu, Zn, Cd, Y, REE and U. Some elements demonstrated non-systematic variation in the course of time for reaction with moss and lichen ash, with a local maxima or both maxima and minima (V, Mn, Cu, Zn, heavy REE, Th). It is possible that a decrease in pH was due to transformation of initial alkali and alkaline-earth hydroxides into carbonates linked to progressive CO_2 uptake from the atmosphere. Such a process has been documented in pine ash (Pereira et al., 2012). However, we could not provide a straightforward explanation for these element temporal patterns and their attribution to either group of solutes. In particular, co-mobilization/precipitation of low solubility "lithogenic" elements (trivalent and tetravalent hydrolysates, Pb) could occur in the form of Al and Fe hydroxide colloids, stabilized by a polymerized (highly aromatic) organic matter that is released from ash material or already present in natural lake water. This is confirmed by positive correlations ($R_P \geq 0.80, p < 0.05$) observed among these elements in experimental leachates (**Table S3**) and is consistent with observations of organo-ferric organo-aluminium colloids which act as carriers of lithogenic elements in surface waters of permafrost peatlands (Pokrovsky et al., 2016). Note that a decrease of lake water DOC and an increase in $SUVA_{254}$ (Fig. 3**G**, **H**) in the presence of all three substrates suggest a sizable adsorption of essentially aliphatic (non-aromatic) dissolved organic matter on ash minerals. As a result, aromatic, highly polymerized DOC remains in the leachate and can stabilize Fe-Al-rich colloids.

To summarize, there are multiple physico-chemical processes shaping the aqueous solution chemistry in the presence of ash material, which include: mineral dissolution and precipitation, adsorption/desorption and co-precipitation. These processes are highly sensitive to both the solution pH and major element concentrations because the latter determine the overall solution saturation state with relevant solid phases. However, under static conditions of batch (closed) reactors used in the present study, one cannot identify specific mechanisms controlling element release rate as a function of time and chemical composition of aqueous solution. To distinguish the impact of solution chemistry (pH, element concentration) and relative reactivity of different solid phases, mixed-flow or column leaching dynamic experiments are necessary.

4.3. Comparison of reactivity of various ashes

Both aqueous solutions used in laboratory leaching experiments – Milli-Q water and DOC-rich natural lake water – exhibited similar element release patterns with the majority of elements mobilized to the aqueous solution within 100 min. Thus, ash produced by tundra burning is highly reactive when in contact with both atmospheric precipitates (rain, snow water) and DOM-rich surface waters (thaw ponds, depressions, suprapermafrost waters). Regardless of the DOC level, there was no sizable difference in pH values of solutions interacting with moss ash (10 to 8) and lichen/peat ash (6 to 5). Because pH is the main factor controlling dissolution of most oxides and carbonates which constitute the ash material (Schott et al., 2009), we therefore conclude that the complexation of trace metal with DOM of lake water did not affect release of these metals from the ash material. This is consistent with results of laboratory experiments, which demonstrated a lack of natural DOM impact on dissolution rates of Ca, Mg oxides, carbonates, and silicates (Pokrovsky et al., 2021 and references therein).

Compared to lichen and peat ash, moss ash exhibited the highest yield of most macro- and micro-nutrients. This was due to a high initial concentration of these elements in the solid phase (see Section 4.1) and a high pH of the contact solution (which presumably stemmed from high concentration of alkali and alkaline-earth metal hydroxides in moss ash). Furthermore, desorption of oxyanions (P, Mo, As, Sb) from mineral surfaces also increases with the pH of solution (Stumm and Morgan, 1995). Note that under such alkaline conditions, we observed exceptional mobility of Al, but not other trivalent hydrolysates, due to the dominance of $Al(OH)_4^-$ soluble hydroxo-complexes at pH levels over 9. Uranium could also become highly mobile in the form of its hydroxo- and carbonate complexes.

At the same time, lichen ash demonstrated 5 to 10 times higher release of P, Fe, light REE and Pb and 2–3 times higher release of Zn and Cd compared to moss ash. While atmospherically deposited heavy metals might be preferentially accumulated in lichen biomass compared to moss biomass (González et al., 2016; Fortuna et al., 2021), enrichment in phosphorus and trivalent cations may be due to some phosphate minerals accumulating in lichens via cyanobacterial symbionts. The prevalence of alkaline-earth metals (Ca, Sr and Ba) in peat ash leachate (as compared to moss ash leachate) may reflect enhanced reactivity of carbonate minerals at 5–4 units lower pH of the peat ash experiments. This could be due to rapidly dissolving carbonate minerals that incorporated these cations.

It is important to note that the highest release of macro- and micronutrients from moss ash—as compared to the lichen and peat ash—is consistent with recent results of field mesocosm experiments where the same 3 main organic substrates (i.e., moss, lichen and peat) of permafrost peatlands were separately added in similar proportions to experimental tanks of thermokarst lake water (Shirokova et al., 2021). These experiments demonstrated that mass-normalized release of DOC, macro-nutrients (Si, N and P), major cations, micro-nutrients and trace metals were essentially controlled by moss and, to a lesser degree, lichen with peat having almost negligible impact. Shirokova et al. (2021) concluded that in contrast to the dominant view of the primary role of peat thaw in controlling element

biogeochemical cycles in permafrost regions in the context of climate warming, the change in vegetation coverage [notably moss/lichen competition] may be a governing factor for element delivery from land to aquatic systems. Results of this work confirm the overwhelming importance, on a mass-normalized scale, of moss ash reactivity in providing macro- and micro-nutrients to surface waters.

4.4. Weak impact of peatland fire on element fluxes and pools in waters

In typical natural environments subjected to wildfire, the mobilization of ash constituents from soil to surface waters is limited by water availability after a fire event, given the relatively arid climate conditions (i.e., Bodí et al., 2014). It has been shown that degrading soot (condensed volatiles) and char (solid organic residue) can move downward into the peat matrix (Certini, 2005; Preston and Schmidt, 2006; Flannigan et al., 2009; Olefeldt et al., 2013) thereby transferring inorganic and organic nutrients back into the soil (Ackley et al., 2021). Furthermore, in the majority of temperate and subtropical settings where wildfires occur, ash leachate products can be transported into groundwater (Hauer and Spencer, 1998; Bodí et al., 2014). These factors (water/moisture limitation and alternative pathways) certainly decrease the potential impact of wildfire on element delivery to the hydrological network. The permafrost nature of the Siberian tundra presents a stark contrast to these settings due to excessive precipitation (especially at the end of the active seasons) and impermeable permafrost layers that allow rapid, complete and (essentially surface) suprapermafrost flow-mediated transport of ash constituents to adjacent thermokarst lakes and draining rivers. In these conditions, the entire amount of elements present in leachable form in ash produced by burnt surface peat and ground vegetation can be mobilized into hydrological network.

The mass balance calculations provided in Section 3.3 (Fig. 5) present the most conservative scenario given that the ash produced from dwarf shrubs, grasses and forest floor litter burning is not included in the leachable stock and that the peat is burned only to a depth of 10 cm. Furthermore, a fire return interval of 56 years for permafrost palsa peatland, based on past decades of monitoring and paleo-reconstructions, may become much shorter in the coming years due to Pan-Arctic increases in summer heat waves and wildfire frequency at higher latitudes (Rocha et al., 2012). Thus, in Arctic tundra, wildfire is projected to increase 4- to 11-fold by 2100 due to increased temperature, evapotranspiration, ignition sources, and vegetation shifts (Abbott et al., 2016; Hu et al., 2010, 2015). Nevertheless, mass balance calculations performed in the present study suggest that even in the case of 10-fold increase in wildfire frequency (and thus, a decreased fire return interval of 5–6 years), its impact on annual element export by tundra rivers will not exceed 10 to 20 %. Such a small increase is within the uncertainties of river solute annual yield quantification. Moreover, even for the case of minimal territory coverage by lakes (4 %), the ash dissolution in surface waters due to the 10-fold increase in wildfire frequency will not impact the concentration of most elements in thermokarst lake waters >10–20 %, with the exception of likely Ca and PO_4. The later finding is consistent with well documented wildfire impact on P export in forested watersheds (Burke et al., 2005). At the same time, the effects of tundra wildfire may be drastically more important on a scale of a single burning event (i.e., Carignan et al., 2000), which can double the concentrations and export fluxes of most major and micro-nutrients for a particular year. In this regard, there is a clear need for further investigation of the significantly understudied reactivity of ash produced by burning of the tundra and forest-tundra zone organic litter horizons, deeper (>10 cm) peat horizons, as well as individual species of grasses and dwarf shrubs.

At the same time, one has to keep in mind the restricted scale of experiments which were aimed solely to quantify to which degree the wildfire in permafrost peatland ecosystems can affect nutrient mobility from the burned soil/peat to the adjacent hydrological network. In particular, our approach ignores particulate emissions (PM2.5) present in smoke and soot, which would be mobilized in dryfall in the form of highly soluble compounds and thus enhance the overall impact of wildfire on surrounding aquatic ecosystems. Furthermore, on a broader scale, the main mechanisms for wildfire effects on biogeochemistry have to deal with altered albedo due to particles deposition from combustion, changes in the depth of the active layer, vegetation and soil moisture — all of which affect microbial activity and nutrient mineralization and mobility (cf., Jafarov et al., 2013).

5. Conclusions

Mosses, lichens, and peat represent the dominant organic substrates in permafrost peatlands subjected to wildfire. Interactions between ash derived from these materials and distilled and natural organic-rich thermokarst lake water were analyzed to assess element release into aqueous solutions. Results of these experiments demonstrated that the majority of solutes (>80–90 %) were leached over the first 10 min of reaction. This suggests virtually instantaneous release of ash constituents into aqueous solution. In accord with the first hypothesis of this study, moss ash is by far the most reactive substance. Moss ash was capable of increasing the pH from 8 to 10 while largely controlling concentrations of soluble highly mobile elements (anions and oxyanions [DIC, Cl, SO_4, B, Mo, Se and Sb], alkalis [Na, K, Rb and Cs], Mg, numerous micronutrients [B, Cu, Mn, Co, Ni, V, Mo and Se] and other trace elements [Al, Sb and U]. The enhanced mobility of oxyanions in moss ash might be due to the alkaline environment of aqueous solution promoting hydrolysis (Al and U^{VI}) or oxyanion desorption from ash particles. Alternatively, lichen ash dissolution affected Si, P and the majority of low solubility hydrolysates [Fe, Y, Zr, Th and REEs] and atmosphere originated pollutants (Zn, Pb and Bi). This is likely due to preferential accumulation of lithogenic minerals, solid aerosols and/or formation of phosphate minerals in their tissues. Finally, peat ash released the highest amounts of Ca, Sr and Ba. This may be linked to enhanced dissolution of carbonate minerals given the rather acidic environments of solutions in which peat ash reacted.

The experimental results did not confirm the second hypothesis of this study, on the importance of tundra wildfire in element cycling in aquatic systems. Despite the very high reactivity of mosses, lichens and peat ash in surface waters, mass balance calculations (factoring in actual vegetation and peat stock of permafrost peatlands and typical regional wildfire frequency) demonstrate that the impact of burning on the element yield of rivers or the element storage of thermokarst lakes is negligibly small. Even a drastic (10-fold) increase in wildfire frequency cannot sizably (>10–20 %) modify macro- and micro-nutrient delivery to the hydrological network (except in the case of Ca and P for lakes). However, the estimations performed in the present work represent a limited, on-side approach to much complex problem of fire event in tundra ecosystems. This highlights the need for further experimental studies on ash derived from forest litter, dwarf shrubs, grasses and perhaps deeper peat horizons in permafrost peatlands.

CRediT authorship contribution statement

Daria Kuzmina: Writing – review & editing, Funding acquisition, Methodology, Data curation. **Artem G. Lim:** Methodology, Data curation. **Sergey V. Loiko:** Investigation. **Oleg S. Pokrovsky:** Conceptualization, Writing – review & editing, Funding acquisition, Investigation.

Data availability

Data will be made available on request.

Declaration of competing interest

The authors declare that they have no known competing financial interests or personal relationships that could have appeared to influence the work reported in this paper.

Acknowledgements

The reported study was funded by RFBR and Yamalo-Nenets Autonomous Okrug, project No 19-44-890013, the RFBR grant No 21-54-75001, and the TSU Development Program “Priority-2030”. We thank two anonymous reviewers for their very thorough and constructive reviews.

Appendix A. Supplementary data

Supplementary data to this article can be found online at https://doi.org/10.1016/j.scitotenv.2022.158701.

References

Abbott, B.W., Jones, J.B., Schuur, E.A.G., et al., 2016. Biomass offsets little or none of permafrost carbon release from soils, streams, and wildfire: an expert assessment. Environ. Res. Lett. 11, 34014. https://doi.org/10.1088/1748-9326/11/3/034014.

Abbott, B.W., Rocha, A.V., Shogren, A., Zarnetske, J.P., Iannucci, F., et al., 2021. Glob. Chang. Biol. 27, 1408–1430. https://doi.org/10.1111/gcb.15507.

Ackley, C., Tank, S.E., Haynes, K.M., Rezanezhad, F., McCarter, C., Quinton, W.L., 2021. Coupled hydrological and geochemical impacts of wildfire in peatland-dominated regions of discontinuous permafrost. Sci. Total Environ. 782, 146841.

Agafontsev, N.V., Kasymov, D.P., 2020. Estimation of the parameters of combustion of the surface of natural combustible materials by the thermography method. J. Eng. Physics Thermophys. 93 (4), 998–1003. https://doi.org/10.1007/s10891-020-02200-w.

Ala-aho, P., Soulsby, C., Pokrovsky, O.S., Kirpotin, S.N., Karlsson, J., Serikova, S., Vorobyev, S.N., Manasypov, R.M., Loiko, S., Tetzlaff, D., 2018. Using stable isotopes to assess surface water source dynamics and hydrological connectivity in a high-latitude wetland and permafrost influenced landscape. J. Hydrol. 556, 279–293. https://doi.org/10.1016/j.jhydrol.2017.11.024.

Bayley, S.E., Schindler, D.W., Beaty, K.G., Parker, B.R., Stainton, M.P., 1992. Effects of multiple fires on nutrient yields from streams draining boreal forest and fen watersheds: nitrogen and phosphorus. Can. J. Fish. Aquatic Sci. 49, 584–596.

Beilman, D.W., MacDonald, G.M., Smith, L.C., Reimer, P.J., 2009. Carbon accumulation in peatlands of West Siberia over the last 2000 years. Glob. Biogeochem. Cycl. 23, GB1012. https://doi.org/10.1029/2007GB003112.

Benscoter, B.W., Thompson, D.K., Waddington, J.M., Flannigan, M.D., Wotton, B.M., de Groot, W.J., Turetsky, M.R., 2011. Interactive effects of vegetation, soil moisture and bulk density on depth of burning of thick organic soils. Internat. J. Wildland Fire 20, 418–429. https://doi.org/10.1071/WF08183.

Boby, L.A., Schuur, E.A.G., Mack, M.C., Verbyla, D., Johnstone, J.F., 2010. Quantifying fire severity, carbon, and nitrogen emissions in Alaska's boreal forest. Ecol. Appl. 20, 1633–1647. https://doi.org/10.1890/08-2295.1.

Bodí, M.B., Martin, D.A., Balfour, V.N., Santín, C., Doerr, S.H., Pereira, P., Cerdá, A., Mataix-Solera, J., 2014. Wildland fire ash: production, composition and eco-hydro-geomorphic effects. Earth Sci. Rev. 130, 103–127. https://doi.org/10.1016/j.earscirev.2013.12.007.

Botch, M.S., Kobak, K.I., Vinson, T.S., Kolchugina, T.P., 1995. Carbon pools and accumulation in peatlands of the former Soviet Union. Glob. Biogeochem. Cycl. 9, 37–46. https://doi.org/10.1029/94GB03156.

Burd, K., Tank, S.E., Dion, N., Quinton, W.L., Spence, C., Tanentzap, A.J., Olefeldt, D., 2018. Seasonal shifts in export of DOC and nutrients from burned and unburned peatland-rich catchments, Northwest Territories, Canada. Hydrol. Earth Syst. Sci. Discuss., 1–32 https://doi.org/10.5194/hess-2018-253.

Burke, J.M., Prepas, E.E., Pinder, S., 2005. Runoff and phosphorus export patterns in large forested watersheds on the western Canadian Boreal Plain before and for 4 years after wildfire. J. Environ. Eng. Sci. 4, 319–325. https://doi.org/10.1139/s04-072.

Carignan, R., D'Arcy, P., Lamontagne, S., 2000. Comparative impacts of fire and forest harvesting on water quality in boreal shield lakes. Can. J. Fish. Aquat. Sci. 57 (Suppl. 2), 105–117. https://doi.org/10.1139/f00-125.

Certini, G., 2005. Effects of fire on properties of forest soils: a review. Oecologia 143, 1–10. https://doi.org/10.1007/s00442-004-1788-8.

Chen, Y., Hu, F., Lara, M., 2021. Divergent shrub-cover responses driven by climate, wildfire, and permafrost interactions in Arctic tundra ecosystems. Glob. Chang. Biol. 27, 652–663. https://doi.org/10.1111/gcb.15451.

Christensen, N.L., 1973. Fire and the nitrogen cycle in California chaparral. Science 181 (4094), 66–68. https://doi.org/10.1126/science.181.4094.66.

Czimczik, C.I., Preston, C.M., Schmidt, M.W.I., Schulze, E.-D., 2003. How surface fire in siberian scots pine forests affects soil organic carbon in the forest floor: stocks, molecular structure, and conversion to black carbon (charcoal). Glob. Biogeochem. Cycl. 17 (1). https://doi.org/10.1029/2002GB001956.

de Groot, W.J., Cantin, A.S., Flannigan, M.D., Soja, A.J., Gowman, L.M., Newbery, A., 2013. A comparison of Canadian and Russian Boreal Forest fire regimes. For. Ecol. Manag. 294, 23–34. https://doi.org/10.1016/j.foreco.2012.07.033.

Diemer, L.A., Mcdowell, W.H., Wymore, A.S., Prokushkin, A.S., 2015. Nutrient uptake along a fire gradient in boreal streams of Central Siberia. Freshwater Sci. 34, 1443–1456. https://doi.org/10.1086/683481.

Dvornikov, Y., Novenko, E., Korets, M., Olchev, A., 2022. Wildfire dynamics along a north-central siberian latitudinal transect assessed using landsat imagery. Remote Sens. 14 (3), 790. https://doi.org/10.3390/rs14030790.

Fang, X., Jia, L., 2012. Experimental study on ash fusion characteristics of biomass. Bioresour. Technol. 104, 769–774. https://doi.org/10.1016/j.biortech.2011.11.055.

Flannigan, M.D., Stocks, B.J., Wotton, B.M., 2000. Climate change and forest fires. Sci. Total Environ. 262, 221–229. https://doi.org/10.1016/S0048-9697(00)00524-6.

Flannigan, M., Stocks, B., Turetsky, M., Wotton, M., 2009. Impacts of climate change on fire activity and fire management in the circumboreal forest. Glob. Chang. Biol. 15, 549–560. https://doi.org/10.1111/j.1365-2486.2008.01660.x.

Fortuna, L., González, A.G., Tretiach, M., Pokrovsky, O.S., 2021. Influence of secondary metabolites on surface chemistry and metal adsorption of a devitalized lichen biomonitor. Environ. Pollut. 273, 116500. https://doi.org/10.1016/j.envpol.2021.116500.

Gibson, C.M., Chasmer, L.E., Thompson, D.K., Quinton, W.L., Flannigan, M.D., Olefeldt, D., 2018. Wildfire as a major driver of recent permafrost thaw in boreal peatlands. Nat. Commun. 9 (1). https://doi.org/10.1038/s41467-018-05457-1.

González, A.G., Pokrovsky, O., Beike, A.K., Reski, R., Di Palma, A., et al., 2016. Metal and proton adsorption capacities of natural and cloned sphagnum mosses. J. Colloid Interface Sci. 461, 326–334. https://doi.org/10.1016/j.jcis.2015.09.012.

Gray, D.M., Dighton, J., 2006. Mineralization of forest litter nutrients by heat and combustion. Soil Biol. Biochem. 38, 1469–1477. https://doi.org/10.1016/j.soilbio.2005.11.003.

Grier, C.C., 1975. Wildfire effects on nutrient distribution and leaching in a coniferous ecosystem. Can. J. For. Res. 5, 599–607. https://doi.org/10.1139/x75-087.

Hanes, C., Wang, X., Jain, P., Parisien, M.-A., Little, J., Flannigan, M.D., 2019. Fire regime changes in Canada over the last half century. Can. J. For. Res. 49 (3), 256–259. https://doi.org/10.1139/cjfr-2018-0293.

Harden, J.W., Neff, J.C., Sandberg, D.V., Turetsky, M.R., Ottmar, R., Gleixner, G., et al., 2004. Chemistry of burning the forest floor during the FROSTFIRE experimental burn, interior Alaska, 1999. Glob. Biogeochem. Cycl. 18. https://doi.org/10.1029/2003GB002194.

Hauer, F.R., Spencer, C.N., 1998. Phosphorus and nitrogen dynamics in streams associated with wildfire: a study of immediate and long-term effects. Int. J. Wildland Fire 8 (4), 183–198. https://doi.org/10.1071/WF9980183.

Heim, R.J., Yurtaev, A., Bucharova, A., Heim, W., Kutskir, V., Knorr, K.-H., Lampei, C., Pechkin, A., Schilling, D., Sulkarnaev, F., Hölzel, N., 2021. Fire in lichen-rich subarctic tundra changes carbon and nitrogen cycling between ecosystem compartments but has minor effects on stocks. Biogeosci. Discuss. https://doi.org/10.5194/bg-19-2729-2022 [preprint].

Heimburger, A., Tharaud, M., Monna, F., Losno, R., Desboeufs, K., Nguyen, E.B., 2013. SLRS-5 elemental concentrations deduced from SLRS-5/SLRS-4 ratios of thirty-three uncertified elements. Geostand. Geoanalytical Res. 37, 77–85. https://doi.org/10.1111/j.1751-908X.2012.00185.x.

Hu, F.S., Higuera, P.E., Walsh, J.E., Chapman, W.L., Duffy, P.A., Brubaker, L.B., Chipman, M.L., 2010. Tundra burning in Alaska: linkages to climatic change and sea ice retreat. J. Geophys. Res. 115, G04002. https://doi.org/10.1029/2009JG001270.

Hu, F.S., Higuera, P.E., Duffy, P., Chipman, M.L., Rocha, A.V., Young, A.M., Kelly, R., Dietze, M.C., 2015. Arctic tundra fires: natural variability and responses to climate change. Front. Ecol. Environ. 13, 369–377. https://doi.org/10.1890/150063.

Ivanova, G.A., Conard, S.G., Kukavskaya, E.A., McRae, D.J., 2011. Fire impact on carbon storage in light conifer forests of the Lower Angara region, Siberia. Environ. Res. Lett. 6 (045203), 1–6. https://doi.org/10.1088/1748-9326/6/4/045203.

Jafarov, E.E., Romanovsky, V.E., Genet, H., McGuire, A.D., Marchenko, S.S., 2013. The effects of fire on the thermal stability of permafrost in lowland and upland black spruce forests of interior Alaska in a changing climate. Environ. Res. Lett. 8, 035030. https://doi.org/10.1088/1748-9326/8/035030.

Kasischke, E.S., Turetsky, M.R., 2006. Recent changes in the fire regime across the north american boreal region-spatial and temporal patterns of burning across Canada and Alaska. Geophys. Res. Lett. 33, 1–5. https://doi.org/10.1029/2006GL025677.

Kasischke, E.S., Hyer, E.J., Novelli, P.C., Bruhwiler, L.P., French, N.H.F., Sukhinin, A.I., Hewson, J.H., Stocks, B.J., 2005. Influences of boreal fire emissions on Northern Hemisphere atmospheric carbon and carbon monoxide. Glob. Biogeochem. Cycl. 19, GB1012. https://doi.org/10.1029/2004GB002300.

Kasischke, E.S., Verbyla, D.L., Rupp, T.S., McGuire, A.D., Murphy, K.A., Jandt, R., Allen, J.A., Hoy, E.E., Duffy, P.A., Calef, M., Turetsky, M.R., 2010. Alaska's changing fire regime – implications for the vulnerability of its boreal forests. Can. J. For. Res. 40, 1313–1324. https://doi.org/10.1139/X10-098.

Kaufmann, J.B., Sanford Jr., R.L., Cummings, D.L., Salcedo, I.H., Sampaio, E.V.S.B., 1993. Biomass and nutrient dynamics associated with slash fires in neotropical dry forests. Ecology 74, 140–151. https://doi.org/10.2307/1939509.

Kawahigashi, M., Prokushkin, A., Sumida, H., 2011. Effect of fire on solute release from organic horizons under larch forest in central Siberian permafrost terrain. Geoderma 166, 171–180. https://doi.org/10.1016/j.geoderma.2011.07.027.

Kharuk, V.I., Ponomarev, E.I., Ivanova, G.A., Dvinskaya, M.L., Coogan, S.C.P., Flannigan, M.D., 2021. Wildfires in the Siberian taiga. Ambio 1–22. https://doi.org/10.1007/s13280-020-01490-x.

Knorre, A.A., Kirdyanov, A.V., Prokushkin, A.S., Krusic, P.J., Büntgen, U., 2019. Tree ring-based reconstruction of the long-term influence of wildfires on permafrost active layer dynamics in Central Siberia. Sci. Total Environ. 652, 314–319. https://doi.org/10.1016/j.scitotenv.2018.10.124.

Köster, E., Köster, K., Berninger, F., Prokushkin, A., Aaltonen, H., Zhou, X., Pumpanen, J., 2018. Changes in fluxes of carbon dioxide and methane caused by fire in Siberian boreal forest with continuous permafrost. J. Environ. Manag. 228, 405–415. https://doi.org/10.1016/j.jenvman.2018.09.051.

Kosykh, N.P., Koronatova, N.G., Naumova, N.B., Titlyanova, A.A., 2008. Above- and below-ground phytomass and net primary production in boreal mire ecosystems of Western Siberia. Wetl. Ecol. Manag. 16 (2), 139–153. https://doi.org/10.1007/s11273-007-9061-7.

Koyama, A., Kavanagh, K.L., Stephan, K., 2010. Wildfire effects on soil gross nitrogen transformation rates in coniferous forests of Central Idaho, USA. Ecosystems 13, 1112–1126. https://doi.org/10.1007/s10021-010-9377-7.

Lamontagne, S., Carignan, R., D'Arcy, P., Prairie, Y.T., Pare´, D., 2000. Element export in runoff from eastern Canadian Boreal Shield drainage basins following forest harvesting and wildfires. Can. J. Fish. Aquatic Sci. 57 (S2), 118–128. https://doi.org/10.1139/f00-108.

Larjavaara, M., Berninger, F., Palviainen, M., Prokushkin, A., Wallenius, T., 2017. Postfire carbon and nitrogen accumulation and succession in Central Siberia. Sci. Rep. 7, 12776. https://doi.org/10.1038/s41598-017-13039-2.

Li, G., Gao, L., Liu, F., Qiu, M., Dong, G., 2022. Quantitative studies on charcoalification: physical and chemical changes of charring wood. Fundam. Res. https://doi.org/10.1016/j.fmre.2022.05.014.

Liljedahl, A., Hinzman, L., Busey, R., Yoshikawa, K., 2007. Physical short-term changes after a tussock tundra fire, Seward Peninsula. Alaska. J. Geophys. Res. Earth Surf. 112, F02S07. https://doi.org/10.1029/2006JF000554.

Ludwig, S.M., Alexander, H.D., Kielland, K., Mann, P.J., Natali, S.M., Ruess, R.W., 2018. Fire severity effects on soil carbon and nutrients and microbial processes in a siberian larch forest. Glob. Chang. Biol. 24, 5841–5852. https://doi.org/10.1111/gcb.14455.

Manasypov, R.M., Shirokova, L.S., Pokrovsky, O.S., 2017. Experimental modeling of thaw lake water evolution in discontinuous permafrost zone: role of peat, lichen leaching and ground fire. Sci. Total Environ. 580, 245–257. https://doi.org/10.1016/j.scitotenv.2016.12.067.

Manasypov, R.M., Lim, A.G., Krickov, I.V., Shirokova, L.S., Vorobyev, S.N., Kirpotin, S.N., Pokrovsky, O.S., 2020. Spatial and seasonal variations of C, nutrient, and metal concentration in Thermokarst lakes of Western Siberia across a permafrost gradient. Water (Switzerland) 12, 1830. https://doi.org/10.3390/w12061830.

Miner, K.R., Turetsky, M.R., Malina, E., Bartsch, A., Tamminen, J., McGuire, A.D., et al., 2022. Permafrost carbon emissions in a changing Arctic. Nat. Rev. Earth Environ. 3, 55–67. https://doi.org/10.1038/s43017-021-00230-3.

Moilanen, M., Silfverberg, K., Hokkanen, T.J., 2002. Effects of wood-ash on the growth, vegetation and substrate quality of a drained mire: a case study. For. Ecol. Manag. 171, 321–338. https://doi.org/10.1016/S0378-1127(01)00789-7.

Morgalev, Y.N., Lushchaeva, I.V., Morgaleva, T.G., Kolesnichenko, L.G., Loiko, S.V., Krickov, I.V., Lim, A., Raudina, T.V., Volkova, I.I., Shirokova, L.S., Morgalev, S.Y., Vorobyev, S.N., Kirpotin, S.N., Pokrovsky, O.S., 2017. Bacteria primarily metabolize at the active layer/permafrost border in the peat core from a permafrost region in western Siberia. Polar Biol. 40, 1645–1659. https://doi.org/10.1007/s00300-017-2088-1.

Neff, J.C., Harden, J.W., Gleixner, G., 2005. Fire effects on soil organic matter content, composition, and nutrients in boreal interior Alaska. Can. J. For. Res. 35, 2178–2187. https://doi.org/10.1139/x05-154.

Novenko, E.Y., Kupryanov, D.A., Mazei, N.G., Prokushkin, A.S., Phelps, L.N., Buri, A., Davis, B.A.S., 2022. Evidence that modern fires may be unprecedented during the last 3400 years in permafrost zone of Central Siberia, Russia. Environmental Research Letters 17 (2), 025004. https://doi.org/10.1088/1748-9326/ac4b53.

Novikov, S.M., Moskvin, Y.P., Trofimov, S.A., Usova, L.I., Batuev, V.I., Tumanovskaya, S.M., et al., 2009. Hydrology of bog territories of the permafrost zone of western Siberia. BBM Publ. House, St. Petersbourg, p. 535 (in Russian).

Olefeldt, D., Turetsky, M.R., Blodau, C., 2013. Altered composition and microbial versus UV-mediated degradation of dissolved organic matter in boreal soils following wildfire. Ecosystems 16 (8), 1396–1412. https://doi.org/10.1007/s10021-013-9691-y.

Parham, L.M., Prokushkin, F.S., Pokrovsky, O.S., Titov, S.V., Grekova, E., Shirokova, L.S., McDowell, W.H., 2013. Permafrost and fire as regulators of stream chemistry in basins of the Central Siberian Plateau. Biogeochemistry 116, 55–68. https://doi.org/10.1007/s10533-013-9922-5.

Pereira, P., Úbeda, X., Martin, D.A., 2012. Fire severity effects on ash chemical composition and water-extractable elements. Geoderma 191, 105–114. https://doi.org/10.1016/j.geoderma.2012.02.005.

Petrone, K.C., Hinzman, L.D., Shibata, H., Jones, J.B., Boone, R.D., 2007. The influence of fire and permafrost on sub-arctic stream chemistry during storms. Hydrol. Process. 21 (4), 423–434. https://doi.org/10.1002/hyp.6247.

Pokrovsky, O.S., Manasypov, R.M., Loiko, S.V., Shirokova, L.S., 2016. Organic and organo-mineral colloids of discontinuous permafrost zone. Geochim. Cosmochim. Acta 188, 1–20. https://doi.org/10.1016/j.gca.2016.05.035.

Pokrovsky, O.S., Manasypov, R.M., Kopysov, S., Krickov, I.V., Shirokova, L.S., Loiko, S.V., Lim, A.G., Kolesnichenko, L.G., Vorobyev, S.N., Kirpotin, S.N., 2020. Impact of permafrost thaw and climate warming on riverine export fluxes of carbon, nutrients and metals in western Siberia. Water 12, 1817. https://doi.org/10.3390/w12061817.

Pokrovsky, O.S., Shirokova, L.S., Zabelina, S.A., Jordan, G., Benezeth, P., 2021. Weak impact of microorganisms on Ca, Mg-bearing silicate weathering. NPj Mater. Degradation 5, 51. https://doi.org/10.1038/s41529-021-00199-w.

Polishchuk, Y.M., Bogdanov, A.N., Muratov, I.N., Polishchuk, V.Y., Lim, A., Manasypov, R.M., Shirokova, L.S., Pokrovsky, O.S., 2018. Minor contribution of small thaw ponds to the pools of carbon and methane in the inland waters of the permafrost-affected part of western siberian lowland. Environ. Res. Lett. 13 (4), 045002. https://doi.org/10.1088/1748-9326/aab046.

Preston, C.M., Schmidt, M.W.I., 2006. Black (pyrogenic) carbon: a synthesis of current knowledge and uncertainties with special consideration of boreal regions. Biogeosciences 3 (4), 397–420. https://doi.org/10.5194/bg-3-397-2006.

Prokushkin, A., Hagedorn, F., Pokrovsky, O., Viers, J., Kirdyanov, A., Masyagina, O., Prokushkina, M., McDowell, W., 2018. Permafrost regime affects the nutritional status and productivity of larches in Central Siberia. Forests 9 (6), 1–18. https://doi.org/10.3390/f9060314 314.

Rocha, A.V., Loranty, M.M., Higuera, P.E., MacK, M.C., Hu, F.S., Jones, B.M., Breen, A.L., Rastetter, E.B., Goetz, S.J., Shaver, G.R., 2012. The footprint of alaskan tundra fires during the past half-century: implications for surface properties and radiative forcing. Environ. Res. Lett. 7. https://doi.org/10.1088/1748-9326/7/4/044039.

Rodríguez-Cardona, B.M., Coble, A.A., Wymore, A.S., Kolosov, R., Podgorski, D.C., Zito, P., Spencer, R.G.M., Prokushkin, A.S., McDowell, W.H., 2020. Wildfires lead to decreased carbon and increased nitrogen concentrations in upland arctic streams. Sci. Rep. 10, 8722. https://doi.org/10.1038/s41598-020-65520-0.

Schott, J., Pokrovsky, O.S., Oelkers, E.H., 2009. The link between mineral dissolution/ precipitation kinetics and solution chemistry. Thermodynamics and Kinetics of Water–Rock Interaction. 70, pp. 207–258. https://doi.org/10.1515/9781501508462-008.

Shirokova, L.S., Chupakov, A.V., Ivanova, I.S., Moreva, O.Y., Zabelina, S.A., Shutskiy, N.A., Loiko, S.V., Pokrovsky, O.S., 2021. Lichen, moss and peat control of C, nutrient and trace metal regime in lakes of permafrost peatlands. Sci. Total Environ. 782, 146737. https://doi.org/10.1016/j.scitotenv.2021.146737.

Sizov, O., Ezhova, E., Tsymbarovich, P., Soromotin, A., Prihod'ko, N., Petäjä, T., Zilitinkevich, S., Kulmala, M., Bäck, J., Köster, K., 2021. Fire and vegetation dynamics in northwest Siberia during the last 60 years based on high-resolution remote sensing. Biogeosciences 18, 207–228. https://doi.org/10.5194/bg-18-207-2021.

Spencer, C.N., Gabel, K.O., Hauer, F.R., 2003. Wildfire effects on stream food webs and nutrient dynamics in Glacier National Park, USA. For. Ecol. Manag. 178, 141–153. https://doi.org/10.1016/S0378-1127(03)00058-6.

Steenari, B.-M., Schelander, S., Lindqvist, O., 1999. Chemical and leaching characteristics of ash from combustion of coal, peat and wood in a 12 MW CFB – a comparative study. Fuel 78 (2), 249–258. https://doi.org/10.1016/S0016-2361(98)00137-9.

Stumm, W., Morgan, J., 1995. Aquatic Chemistry: Chemical Equilibria and Rates in Natural Waters, 3rd edition Wiley, p. 1040.

Talucci, A.C., Loranty, M.M., Alexander, H.D., 2022. Siberian taiga and tundra fire regimes from 2001–2020. Environ. Research Lett. 17, 025001.

Volkova, I.I., Kolesnichenko, L.G., Volkova, A.I., Obuchova, A.Y., Pokrovsky, O.S., Vorobyev, S.N., 2018. Peat-forming mosses as a key component of peat deposits and mire vegetation in the West Siberian Northern taiga. Mosses: Eclogy, Lide Cycle and Significance, pp. 175–189.

Whelan, R.J., 1995. The Ecology of Fire. Cambridge University Press, USA, p. 346.

White-Monsant, A.C., Clark, G.J., Chuen, M., Camac, J.S., Wang, X., Papst, W.A., Tang, C., 2015. Experimental warming and fire alter fluxes of soil nutrients in sub-alpine open heathland. Clim. Res. 64 (2), 159–171. https://doi.org/10.3354/cr01273.

Wright, H.A., Bailey, A.W., 1982. Fire Ecology: United States and Southern Canada. John Wiley & Sons, New York, p. 501.